Proceedings of the 35th European Safety and Reliability & the 33rd Society for Risk Analysis Europe Conference
Edited by Eirik Bjorheim Abrahamsen, Terje Aven, Frederic Bouder, Roger Flage, Marja Ylönen
 Published by Research Publishing, Singapore.
doi: 10.3850/978-981-94-3281-3_ESREL-SRA-E2025-P5740-cd

The Effect of Random Spatial Variability in Masonry Bricks Unit Material Properties on the Structural Performance of Unreinforced Masonry Walls

Abayomi Owoeye[1], Frederic Duprat[2], Thomas de Larrard[3], Zakaria Djamai[4]

[1,2,3,4]*Université de Toulouse; INSA, LMDC (Laboratoire Matériaux et Durabilité des Constructions); 135, avenue de Rangueil; F-31 077 Toulouse Cedex 04, France.*
[1]Owoeye@insa-toulouse.fr, [2]duprat@insa-toulouse.fr, [3]delarrar@insa-toulouse.fr, [4]djamai@insa-toulouse.fr

This paper presents the numerical analyses aimed at investigating the effect of correlated random fields properties - such as elastic modulus, compression resistance, and deformation at peak compression - of masonry brick units on the in-plane behavior of Unreinforced Masonry (URM) wall using a finite element model (FEM). Non-linear analyses are developed by applying an in-plane horizontal displacement load and iteratively changing the correlated random field material properties of the wall's masonry brick units while keeping the value of the vertical compression stress applied on the wall constant. Firstly, the random field model's reliability is verified by comparing it with an established deterministic model and a documented experimental test result from the literature. The same model is then used to investigate the influence of uncertainties of the material properties of brick units on the global behavior of the URM wall. The random field numerical analysis results show the considerable effect of the spatially varying material properties of masonry brick units on the macro performance of the masonry wall in terms of ultimate strength and failure modes. The results also demonstrate the influence of the cross-correlation between the random fields of masonry brick unit elastic modulus, compression resistance, and tensile resistance on the global behavior of the wall.

Keywords: Masonry, Random fields, Uncertainty propagation, Spatial variability, Cross-correlation.

1. Introduction

Unreinforced masonry (URM) structures are composite and complex systems made from units such as clay bricks, stones, and other natural materials, along with mortar. The capacity and behavior of URM structures are largely influenced by several factors, including the intrinsic characteristics of the URM itself, the quality of workmanship (such as bond patterns and overall construction quality), aging, previous interventions, and the mechanical properties of the constituent materials (units and mortar). (Malomo, DeJong, and Penna 2021; Pulatsu, Bretas, and Lourenco 2016; Napolitano and Glisic 2019; Pulatsu, Gencer, and Erdogmus 2022). These variations (both at the time of construction and throughout the URM lifetime) result in a structural system subject to high spatial variability, thereby influencing the global mechanical response of the system, such as overall force-displacement behavior and ultimate load resistance capacity. In recent times, researchers have explored the spatial variation of unit and mortar joint properties in the computational modeling of masonry walls, examining the extent to which these variations affect the results (Gonen et al. 2022; 2021; Gooch, Masia, and Stewart 2021; Li et al. 2016; Tabbakhha and Deodatis 2017). These studies primarily focus on the variation in material properties between units, with particular emphasis on the mortar and brick/mortar joint interfaces. However, in URM structures, the mechanical properties of the units and mortar vary significantly, especially in traditional hand-made brick, stone, and other forms of natural masonry (Gonen et al. 2022; Gonen and Soyoz 2021; Makoond et al. 2020; Owoeye et al. 2024; Stewart and Heffler 2008).

Building on this foundation, this present study aims to specifically investigate the effect of correlated random fields properties - such as elastic modulus, E_B, compression resistance, RC_B, tension resistance, RT_B and deformation at peak compression, EPC_B - of masonry brick units on the in-plane behavior of URM walls. This investigation employs an optimized three-

dimensional (3D) finite element model (FEM) built in CAST3M (CAST3M 2023) and random field theory, which are considered more realistic for addressing a wide range of structural engineering problems by accommodating the complex, multidimensional, and multivariate nature of randomly varying material properties and characteristics (Vanmarcke et al. 1986). The study draws upon the extensive experimental research conducted by Tarifa (2023).

The following sections discuss the numerical modeling approach, material properties, random field model, model validation, mesh sensitivity analysis, simulation examples and discussion, and relevant conclusions derived from the study.

2. Numerical Modeling

This section describes a 3D nonlinear FEM of a masonry brick wall, with dimensions closely matching those tested by Tarifa (2023). The ENDO3D material behavioral model of FLUENDO3D (Sellier 2018), incorporated within the CAST3M finite element (FE) software environment, was adopted. The CAST3M FE software was used because it allows for incorporating Python-simulated correlated random field material properties for FE analysis.

Using a 3D micro-modeling strategy, the bricks and mortar joints were represented as nonlinear elastic viscoplastic continuum cube elements (element type CUB8). Within the FE model, the components of the masonry wall are classified into four categories (**Fig. 1**): half brick (0.2m × 0.2m × 0.051m), full brick (0.42m × 0.2m × 0.051m), head mortar (0.02m × 0.2m × 0.051m), and bed mortar (0.44m × 0.2m × 0.017m).

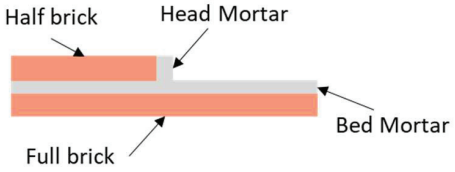

Fig. 1: Model wall components.

Three nodal discretization configurations that included all the wall components were examined to optimize the FE model's mesh refinement and density. **Fig. 2** presents the discretized components of each model category, designated as M1, M2, and M3, and their respective discretization in parenthesis. The dimension of the FE wall model is 1.32m × 0.2m × 1.38m (**Fig. 3**).

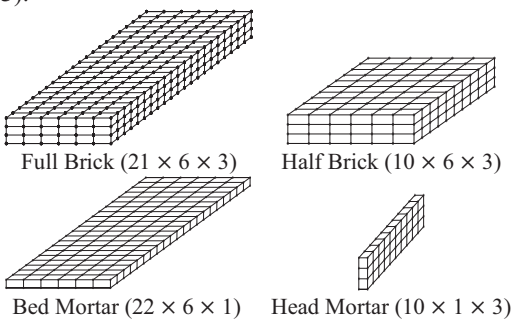

(a) M1 component discretization

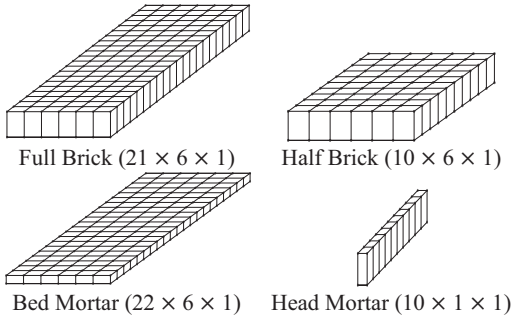

(b) M2 component discretization

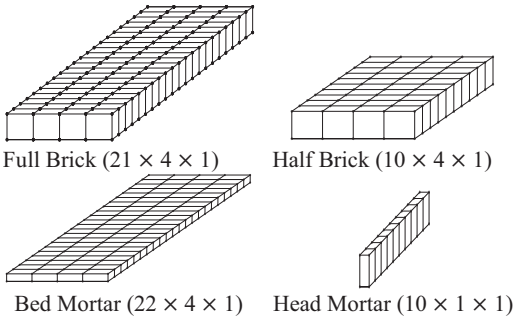

(c) M3 component discretization

Fig. 2: Model components discretization.

A perfect adhesion was assumed at the mortar/brick unit interface to simplify the model and reduce its computational cost. To mimic a monotonic combined in-plane compression-shear behavior (**Fig. 3**), an equivalent of a constant 70kN imposed vertical compression load is applied on the top surface of the masonry wall model. Additionally, an incremental in-plane horizontal displacement load is applied to the top right edge of the wall at a load step of 0.01 (equivalent to 0.00008m horizontal displacement) for a total of 0.008m horizontal in-plane

displacement (a significant displacement above the observable decrease in the magnitude of the experimental applied in-plane load (Tarifa 2023)).

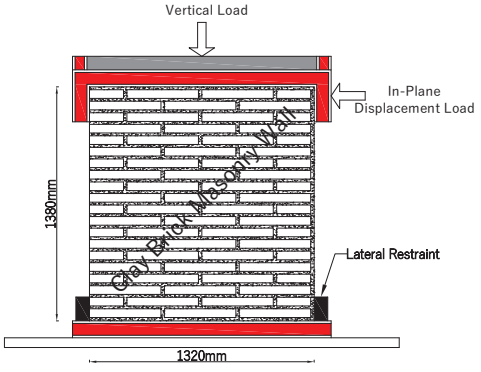

Fig. 3: Illustration of a monotonic combined in-plane compression-shear test setup.

3. Material Properties

The present study is built upon the research conducted by Tarifa (2023), specifically for the URM, URM components and ENDO3D material behavioral model requirement. The research involves a series of laboratory tests that include a monotonic combined in-plane compression-shear laboratory test on an URM brick wall with dimensions 1.32m × 0.2m × 1.38m, compression and bending tests on mortar and bricks samples for ENDO3D behavioral model and material property characterization. The URM masonry wall was built using terracotta bricks like those commonly used for historic buildings in Toulouse. The laboratory tests and results have been extensively documented by Tarifa (2023), and they are not the focus of this study. However, all the necessary information required for the FEM of an URM wall is presented herein. **Table 1** presents the mechanical properties use for the ENDO3D FEM, taken from Tarifa (2023). Note that the parameters presented in **Table 1** are brick and mortar parameters required for the random field FEM. Only the material properties with define Coefficient of Variation (COV) in **Table 1** (i.e., elastic modulus, E_B, compression resistance, RC_B, tension resistance, RT_B and deformation at peak compression, EPC_B) were assumed to be defined by random field, while all other parameters remain constant. The unit brick deformation at peak tension was assumed to be $EPT_B = \frac{RC_B}{E_B}$, while that of the mortar was assumed to follow the relationship, $EPT_M = 1.3 \times \frac{RC_T}{E_T}$.

Table 1: ENDO3D FEM mechanical properties (Tarifa 2023).

Material	Property	Unit	Mean Value	COV
Brick	Elastic modulus, E_B	MPa	7600	21
	Tensile strength, RT_B	MPa	1.000	22
	Compressive strength, RC_B	MPa	13.72	23
	Poisson ratio, NU_B	-	0.150	-
	Deformation at peak compression, EPC_B	-	0.003	33
	Drucker Prager confinement coefficient	-	0.0025	-
Mortar	Elastic modulus, E_M	MPa	2000	-
	Tensile strength, RT_M	MPa	0.02	-
	Compressive strength, RC_M	MPa	1.300	-
	Poisson ratio	-	0.262	-
	Deformation at peak compression, EPC_M	-	0.0032	-
	Drucker Prager confinement coefficient	-	0.38	-

4. Random Field Material Property Model, Cross-Correlation and Simulation

Random field theory was used to describe the spatial variability inherent in the properties (i.e., elastic modulus, E_B, compression resistance, RC_B, tension resistance, RT_B and deformation at peak compression, EPC_B) of the FEM model's unit bricks. All random fields material properties used for the FEM are assumed to follow a Lognormal distribution generated according to Eq. (1).

$$H_i = exp\left(\mu_{N,H_i} + \sigma_{N,H_i} G(x)\right) \quad (1)$$

Where H_i is the spatially varied random material property i, μ_{N,H_i} and σ_{N,H_i} are, respectively, the mean and standard deviation of H_i in the normal space. $G(x)$ is assumed to be a standardized Rational Quadratic (RQ) autocorrelation function in Gaussian space with a unit variance, defined as in Eq. (2).

$$G(x) = \left(1 + \frac{1}{2 \times 1.44}\left(\frac{h}{r}\right)^2\right)^{-1.14} \quad (2)$$

x, is the spatial location (nodes) within the domain of the field defined by the geometry of the component, h is lag distance and $r = 1.54$, is the length scale parameter which controls how quickly the correlation between points decreases with distance (Duvenaud 2014; Hristopulos and Žukovič 2011). The RQ autocorrelation function was employed to define the random fields due to its efficient solution capability, which is particularly effective for interpolating smooth functions over domains where fine-scale variations are significant (Duvenaud 2014). If the parameters μ_{H_i} and σ_{H_i}, respectively, denote the mean and standard deviation of H_i and the coefficient of variation (COV) is $v_{H_i} = \frac{\sigma_{H_i}}{\mu_{H_i}}$, then,

$$\mu_{N,H_i} = \ln\left(\frac{\mu_{H_i}^2}{\sqrt{\mu_{H_i}^2 + \sigma_{H_i}^2}}\right), \sigma_{N,H_i} = \sqrt{\ln\left(1 + \frac{\sigma_{H_i}^2}{\mu_{H_i}^2}\right)}.$$

4.1. *Cross-Correlated Random fields and simulation*

If there are $H_1, H_2, H_3, \ldots, H_n$ cross correlated random fields within the domain, and the random fields share identical standardized autocorrelation function $G(x)$, where $\boldsymbol{C} \in \mathbb{R}^{(n \times n)}$ is the cross-correlation matrix; then according to Vořechovský (2008), $G(x)$ could be expanded as in Eq. (3).

$$G(x) = \sum_{j=1}^{p} V_j \sqrt{\lambda_j} \xi_i(\theta) \quad (3)$$

Where λ_i and V_i are the p non-trivial eigenvalues (arranged in descending order) and corresponding eigenfunctions from a spectral decomposition of $G(x)$ and $\xi_i(\theta) \in \xi^D = [[\xi_1]^T, [\xi_2]^T, [\xi_3]^T, \ldots, [\xi_n]^T,]^T$ is a set of jointly distributed independent random vectors which is estimated as;

$$\xi^D = \sum_{j=1}^{p} V^D \sqrt{\lambda^D} \xi \quad (4)$$

Where; $\boldsymbol{V^D} = \begin{pmatrix} \phi_{1,1}\boldsymbol{I} & \phi_{1,2}\boldsymbol{I} & \cdots & \phi_{1,n}\boldsymbol{I} \\ \phi_{2,1}\boldsymbol{I} & \phi_{2,2}\boldsymbol{I} & \cdots & \phi_{2,n}\boldsymbol{I} \\ \vdots & \vdots & \vdots & \vdots \\ \phi_{n,1}\boldsymbol{I} & \phi_{n,2}\boldsymbol{I} & \cdots & \phi_{n,n}\boldsymbol{I} \end{pmatrix}$, $\boldsymbol{\Lambda^D} = diag\ (\lambda_1\boldsymbol{I}, \lambda_2\boldsymbol{I}, \lambda_3\boldsymbol{I}, \ \ldots, \lambda_n\boldsymbol{I})$, $\boldsymbol{I} \in \mathbb{R}^{p \times p}$ is a $p \times p$ identity matrix, and the values $\phi_{i,j}$, and λ_i are the components eigenfunctions $\boldsymbol{Vec^C} = \begin{pmatrix} \phi_{1,1} & \phi_{1,2} & \cdots & \phi_{1,n} \\ \phi_{2,1} & \phi_{2,2} & \cdots & \phi_{2,n} \\ \vdots & \vdots & \vdots & \vdots \\ \phi_{n,1} & \phi_{n,2} & \cdots & \phi_{n,n} \end{pmatrix}$, and eigenvalues $\boldsymbol{\Lambda^C} = diag\ (\lambda_1, \lambda_2, \lambda_3, \ \ldots, \lambda_n)$ obtained from the spectra decomposition of the cross-correlation matrix $\boldsymbol{C}$, and $\xi \in \mathbb{R}^{p \times n}$ is a $(p \times n)$ independent standard random variable (Vořechovský 2008).

The procedure of simulating the cross-correlated random field material properties at the nodes of each component category of the URM wall could be easily implemented in Python (Rossum, Guido, and Drake 2009) along with its scientific libraries using the material properties and their uncertainties defined in **Table 1**, $G(x)$ and $\boldsymbol{C}$. Two distinct cross-correlations were considered (i.e., a near perfectly correlated and un-correlated unit brick random field material properties) in this study for simulating material properties which then served as input fields for CAST3M FEM and analysis.

5. Model Validation and Mesh Sensitivity Analysis

To validate the model and evaluate the FEMs mesh refinement, a near deterministic model was used by initially setting the Coefficient of

Variations (COV) for all the random fields material properties to 1×10^{-5} and a near perfect cross correlation, $\boldsymbol{C} = 0.9$, that is $\boldsymbol{C} = \begin{bmatrix} [1.0, E\_RC, E\_EPC, E\_RT], \\ [\ldots, 1.0, RC\_EPC, RC\_RT], \\ [\ldots\ldots\ldots\ldots, 1.0, EPC\_RT], \\ [\ldots\ldots\ldots\ldots\ldots\ldots, 1.0] \end{bmatrix} = \begin{bmatrix} [1.0, 0.9, 0.9, 0.9], \\ [0.9, 1.0, 0.9, 0.9], \\ [0.9, 0.9, 1.0, 0.9], \\ [0.9, 0.9, 0.9, 1.0] \end{bmatrix}$, between the properties, was considered. Note that the correlation between E_B and RC_B is E_RC, between E_B and EPC_B is E_EPC, between E_B and RT_B is E_RT and vis-versa.

Presented in **Fig. 4** is the in-plane force displacement curves from the experimental data and the near deterministic models constructed from the component discretization (M1, M2, and M3) in **Fig. 2**

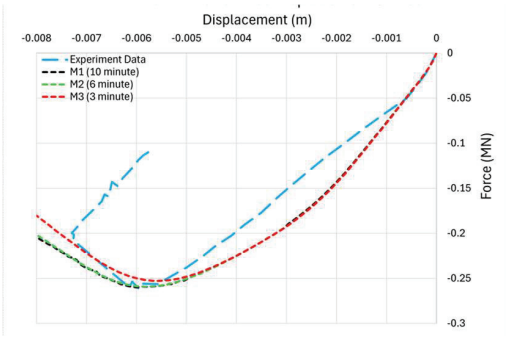

Fig. 4: In-plane force displacement curves from experimental data and model M1, M2 and M3 for $\boldsymbol{C} = 0.9$, and all COV = 1×10^{-5}.

The experimental data revealed two distinct pre-peak slope segments (i.e., between 0 - 0.05MN and 0.05 - 0.26MN). All the near-deterministic models aligned with the first segment, while there was an obvious difference between the experimental data and the models in the second segment. The difference observed in the second segment is due to the assumption of a perfect bond between the mortar/brick interface. The same assumption is responsible for the difference in the post-peak slope of the models and experimental data. Also, it was observed that the finer mesh models, M1 and M2 accurately predict the experiment's peak load and corresponding displacement. Therefore, the optimal model, M2 with analysis duration of six-minute will be adopted for evaluating the effect of random spatial variability in masonry bricks unit material properties on the structural performance of the URM walls.

In addition, like the URM wall tested by Tarifa (2023), all the wall model configurations failed in diagonal shear as shown in **Fig. 5**, for Model M2 tensile damage (scaled 0 – 1: 0 = no damage, 1 = total damage).

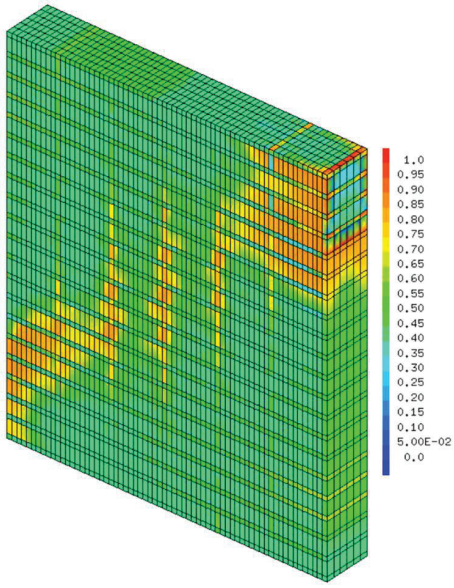

Fig. 5: Model M1 tensile damage,

Once the applicability of the model was established, a series of correlated and uncorrelated unit brick random spatial material properties were generated using Python script, and the effect on the global in-plane response of the URM wall was investigated.

6. Effect of Correlated and Un-Correlated Unit Brick Material Property on URM Response

To investigate the effect of random spatial variability in masonry bricks unit material properties on the structural performance of URM wall using the proposed model, two distinct COV classes were considered; that is using the COV as presented in **Table 1** for E_B, RC_B RT_B, and EPC_B as COV1, and COV2 = (42, 44, 46, 33) for E_B, RC_B RT_B, and EPC_B coefficient of variations

respectively. COV2 is a multiple of COV1 except for the COV of EPC_B. These two classes of COVs were then used to simulate correlated and uncorrelated unit brick random fields material properties using a near perfect cross-correlation and un-correlated cross-correlation respectively.

The near perfect cross correlation is defined as,

$$\boldsymbol{C1} = \begin{bmatrix} [1.0, E\_RC, E\_EPC, E\_RT], \\ [\ldots, 1.0, RC\_EPC, RC\_RT], \\ [\ldots\ldots\ldots\ldots, 1.0, EPC\_RT], \\ [\quad \ldots\ldots\ldots\ldots\ldots\ldots, 1.0] \end{bmatrix} = \begin{bmatrix} [1.0, 0.8, 0.2, 0.8], \\ [0.8, 1.0, 0.2, 0.8], \\ [0.2, 0.2, 1.0, 0.2], \\ [0.8, 0.8, 0.2, 1.0] \end{bmatrix},$$

and

$$\boldsymbol{C2} = \begin{bmatrix} [1.0, E\_RC, E\_EPC, E\_RT], \\ [\ldots, 1.0, RC\_EPC, RC\_RT], \\ [\ldots\ldots\ldots\ldots, 1.0, EPC\_RT], \\ [\quad \ldots\ldots\ldots\ldots\ldots\ldots, 1.0] \end{bmatrix} = \begin{bmatrix} [1.0, 0.2, 0.2, 0.2], \\ [0.2, 1.0, 0.2, 0.2], \\ [0.2, 0.2, 1.0, 0.2], \\ [0.2, 0.2, 0.2, 1.0] \end{bmatrix}$$

is the un-correlated cross-correlation.

It is important to note that in the cross-correlation matrix $\boldsymbol{C1}$, the deformation at peak compression, EPC_B was assumed to be uncorrelated to either of E_B, RC_B, and RT_B.

Presented in **Fig. 6** are the stochastic responses of the URM wall FEM to seventy-five (75) simulated input random field material properties of the unit bricks, combining each COV and cross correlations. Meanwhile, **Fig. 7** presents the Mean of each stochastic response, the experimental data, and the previously computed near-deterministic data.

As can be seen in **Fig. 6**, the stochastic response suggests that an increase in the COV of unit brick material properties significantly increases the variation in the in-plane force-displacement response of the wall and leads to less reliable prediction of the experimental test result. This is evident in **Fig. 7**, where the peak in-plane displacement response and corresponding displacement for the correlated and un-correlated mean stochastic responses using COV2 are lower than that of COV1, experimental test, and the near deterministic result.

Furthermore, the effect of considering cross-correlation between unit brick material properties is more obvious with the higher COV, that is,

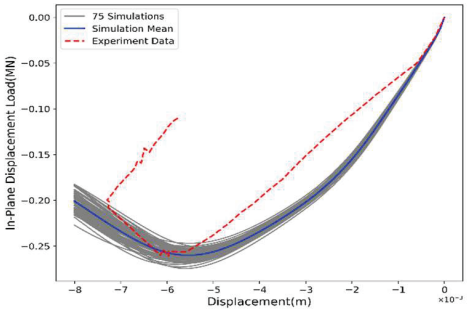

(a) Correlated Brick Properties (COV1 & C1)

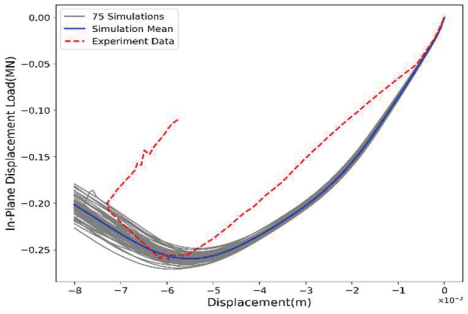

(b) Un-Correlated Brick Properties (COV1 & C2)

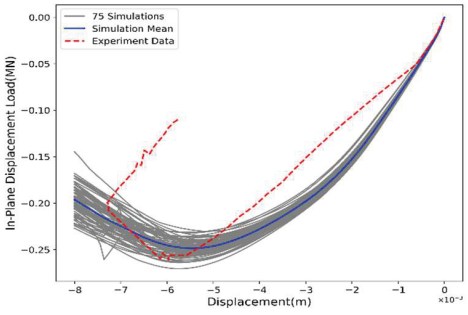

(c) Correlated Brick Properties (COV2 & C1)

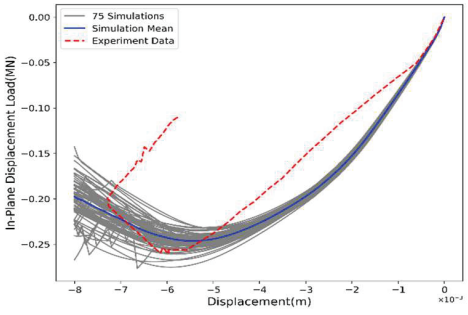

(d) Un-Correlated Brick Properties (COV2 & C2)

Fig. 6: Stochastic response of URM wall to input random field material properties of unit bricks

COV2. However, with the lower COV, that is, COV1, the mean stochastic responses for both correlated (CorrelatedMean (COV1 & C1)) and uncorrelated (UnorrelatedMean (COV1 & C2)) are undistinguishable (**Fig. 7**).

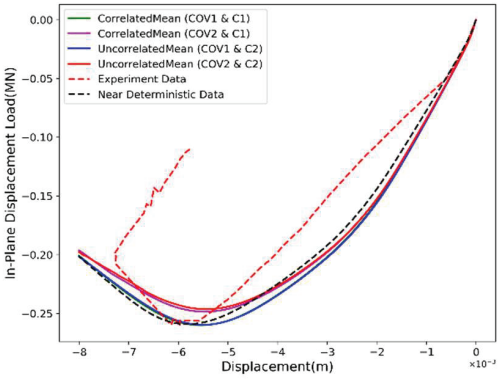

Fig. 7: Stochastic means in-plane force displacement curves.

7. Conclusion

URM structures are complex systems that require extensive experimental and analytical research to achieve a deeper understanding of their behavior. This study presents the effect of considering the correlation between the random field material properties of a masonry brick unit on the global behavior of the URM structure.

The main conclusions of the study can be summarized as follows:

Using random fields to describe the material properties of URM wall unit bricks provides a stochastic result (i.e., Ultimate horizontal resistance strength and corresponding displacement), which can be used for further reliability assessment of the wall.

The correlation between the unit brick random fields material properties has little or no effect on the mean stochastic results. The effect is more pronounced when the COV of the material properties within each brick unit increases to above 45%.

The investigation also suggests that the lower the COV of unit bricks' material properties, the lower the variation in the force-displacement capacity and the closer the numerical models are to the experimental finding.

The present study will be extended to investigate the effect of mortar joints random material properties, the combined effect of mortar joints and unit brick random material properties on the structural response of URM, and stochastic reliability study in the future.

References

CAST3M. 2023. 'Cast3M Theoretical Documentation — Cast3M Documentation - Theory 2023.0'. 2023. https://www-cast3m.cea.fr/html/doc_theo/index.html.

Duvenaud, David. 2014. 'Automatic Model Construction with Gaussian Processes', November. https://doi.org/10.17863/CAM.14087.

Gonen, Semih, Bora Pulatsu, Ece Erdogmus, Paulo B. Lourenço, and Serdar Soyoz. 2022. 'Effects of Spatial Variability and Correlation in Stochastic Discontinuum Analysis of Unreinforced Masonry Walls'. *Construction and Building Materials* 337 (June):127511. https://doi.org/10.1016/j.conbuildmat.2022.127511.

Gonen, Semih, Bora Pulatsu, Serdar Soyoz, and Ece Erdogmus. 2021. 'Stochastic Discontinuum Analysis of Unreinforced Masonry Walls: Lateral Capacity and Performance Assessments'. *Engineering Structures* 238 (July):112175. https://doi.org/10.1016/j.engstruct.2021.112175.

Gonen, Semih, and Serdar Soyoz. 2021. 'Investigations on the Elasticity Modulus of Stone Masonry'. *Structures* 30 (April):378–89. https://doi.org/10.1016/j.istruc.2021.01.035.

Gooch, Lewis J., Mark J. Masia, and Mark G. Stewart. 2021. 'Application of Stochastic Numerical Analyses in the Assessment of Spatially Variable Unreinforced Masonry Walls Subjected to In-Plane Shear Loading'. *Engineering Structures* 235 (May):112095. https://doi.org/10.1016/j.engstruct.2021.112095.

Hristopulos, Dionissios T., and Milan Žukovič. 2011. 'Relationships between Correlation Lengths and Integral Scales for Covariance Models with More than Two Parameters'. *Stochastic Environmental Research and Risk Assessment* 25 (1): 11–19. https://doi.org/10.1007/s00477-010-0407-y.

Li, Jie, Mark G. Stewart, Mark J. Masia, and Steven J. Lawrence. 2016. 'Spatial Correlation of Material Properties and Structural Strength of Masonry in Horizontal Bending'. *Journal of Structural Engineering-Asce* 142:04016112.

Makoond, Nirvan, Albert Cabané, Luca Pelà, and Climent Molins. 2020. 'Relationship between the Static and Dynamic Elastic Modulus of Brick Masonry Constituents'. *Construction and Building Materials* 259 (October):120386. https://doi.org/10.1016/j.conbuildmat.2020.120386.

Makoond, Nirvan, Luca Pelà, and Climent Molins. 2019. 'Dynamic Elastic Properties of Brick

Masonry Constituents'. *Construction and Building Materials* 199 (February):756–70. https://doi.org/10.1016/j.conbuildmat.2018.12.071.

Malomo, D., M.J. DeJong, and A. Penna. 2021. 'Influence of Bond Pattern on the In-Plane Behavior of URM Piers'. *International Journal of Architectural Heritage* 15 (10): 1492–1511. https://doi.org/10.1080/15583058.2019.1702738.

Napolitano, Rebecca, and Branko Glisic. 2019. 'Understanding the Function of Bonding Courses in Masonry Construction: An Investigation with Mixed Numerical Methods'. *Journal of Cultural Heritage* 39 (September):120–29. https://doi.org/10.1016/j.culher.2019.03.007.

Owoeye, A. Owoeye, T. De Larrard Larrard, Z. Djamai Djamai, and F. Duprat Duprat. 2024. 'Brick Masonry Constituent Material Property Characterization Through Impact Excitation and Ultrasonic Pulse Velocity Test.' *9th European Congress on Computational Methods in Applied Sciences and Engineering* New Trends in Computational Modelling of Masonry Material and Structures (October). URL https://www.scipedia.com/public/Owoeye_et_al_2024a.

Pulatsu, Bora, Eduardo M. Bretas, and Paulo B. Lourenco. 2016. 'Discrete Element Modeling of Masonry Structures: Validation and Application'. *Earthquakes and Structures* 11 (4): 563–82. https://doi.org/10.12989/EAS.2016.11.4.563.

Pulatsu, Bora, Funda Gencer, and Ece Erdogmus. 2022. 'Study of the Effect of Construction Techniques on the Seismic Capacity of Ancient Dry-Joint Masonry Towers through DEM'. *European Journal of Environmental and Civil Engineering* 26 (9): 3913–30. https://doi.org/10.1080/19648189.2020.1824823.

Rossum, Van, Guido, and Fred L. Drake. 2009. *Python 3 Reference Manual*. Scotts Valley, CA: CreateSpace.

Sellier, Alain. 2018. 'Anisotropic Damage and Visco-Elasto-Plasticity Applied to Multiphasic Materials'. Research Report. LMDC - Laboratoire Matériaux et Durabilité des Constructions de Toulouse ; Université de Toulouse III - Paul Sabatier ; INSA de Toulouse. https://insa-toulouse.hal.science/hal-01710289.

Stewart, Mark, and Leesa Heffler. 2008. 'Statistical Analysis and Spatial Correlation of Flexural Bond Strength for Masonry Walls'. *Masonry International* 21 (January):57–70.

Tabbakhha, Maryam, and George Deodatis. 2017. 'Effect of Uncertainty of Tensile Strength of Mortar Joints on the Behavior of Masonry Walls under Lateral Loads'. *Journal of Structural Engineering* 143 (2): 04016166. https://doi.org/10.1061/(ASCE)ST.1943-541X.0001640.

Tarifa, Nadia. 2023. 'Renforcement de la maçonnerie historique par les composites TRM'. Phdthesis, INSA de Toulouse. https://theses.hal.science/tel-04523939.

Vanmarcke, E., M. Shinozuka, S. Nakagiri, G. I. Schuëller, and M. Grigoriu. 1986. 'Random Fields and Stochastic Finite Elements'. *Structural Safety* 3 (3): 143–66. https://doi.org/10.1016/0167-4730(86)90002-0.

Vořechovský, Miroslav. 2008. 'Simulation of Simply Cross Correlated Random Fields by Series Expansion Methods'. *Structural Safety* 30 (4): 337–63. https://doi.org/10.1016/j.strusafe.2007.05.002.